Figure S1

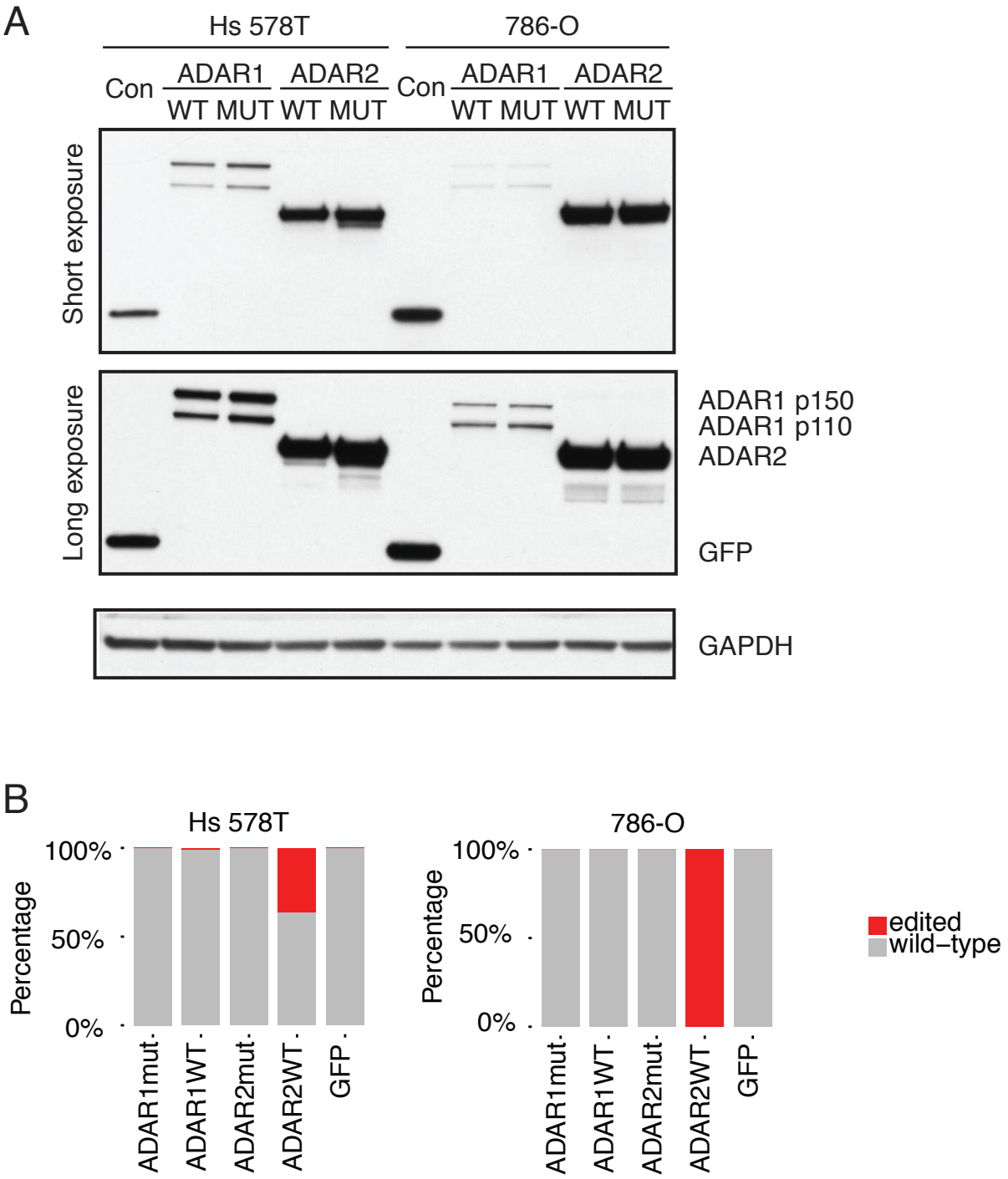

Supplemental Fig. 1. Validation of edited miR-379-5p catalyzed by ADAR2
(A) Western blot of ADAR enzyme overexpression in Hs 578T and 786-O cell lines (NC: negative control, WT: wild-type, MUT: mutated). (B) Changes in miR-379-5p editing level after transfection with different ADAR enzymes.

Figure S2

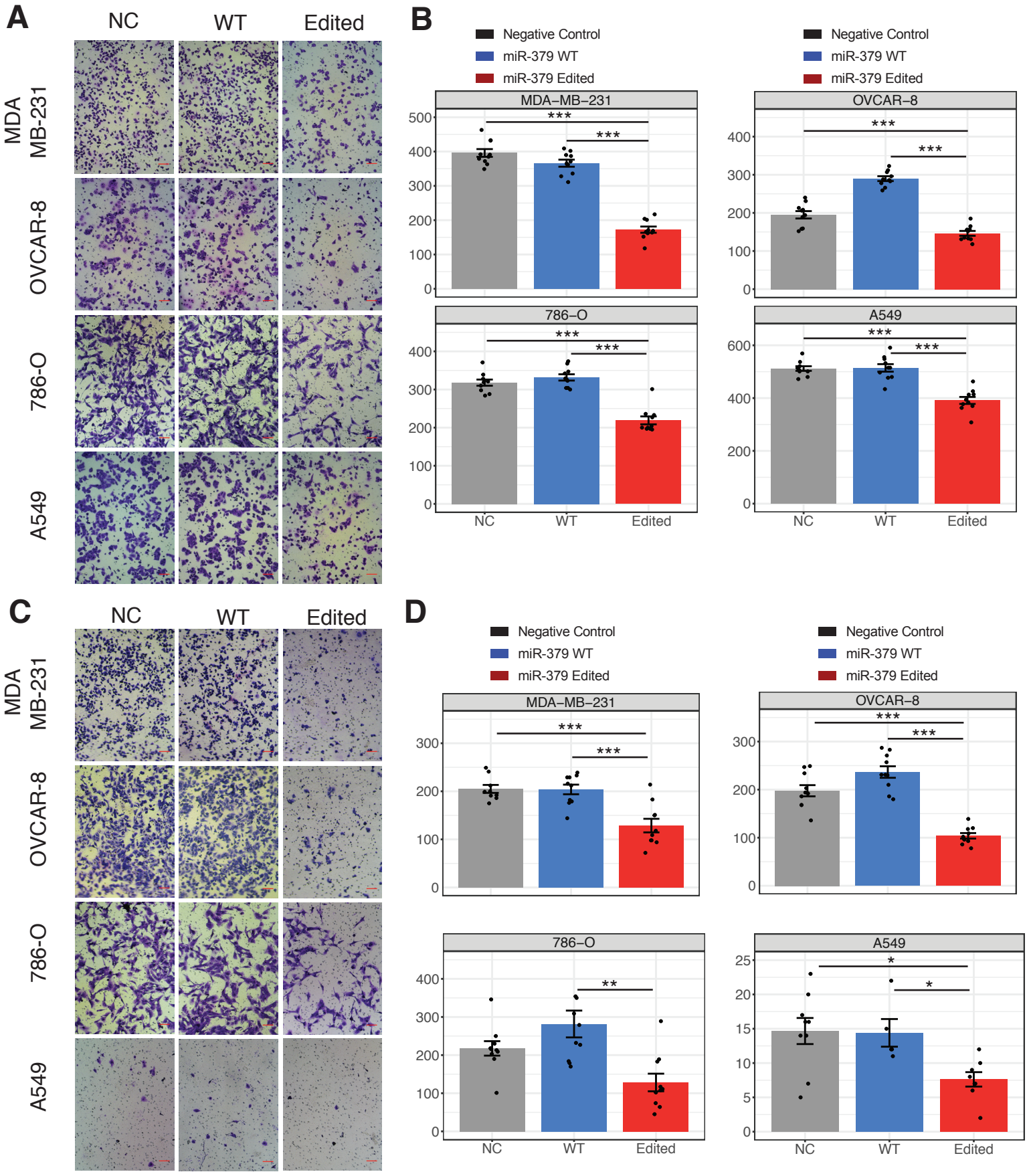

Supplemental Fig. 2. Effects of miRNA editing in miR-379-5p on cell migration and invasion (A-B) migration and (C-D) invasion in MDAMB-231, OVCAR-8, 786-O, and A549 cells. Error bars denote ±SEM; ANOVA with Tukey's test as post-hoc test was used to assess the difference; $*p < 0.05$, $**p < 0.01$, $***p < 0.001$. Scale bar length is 100 μm.

Figure S3

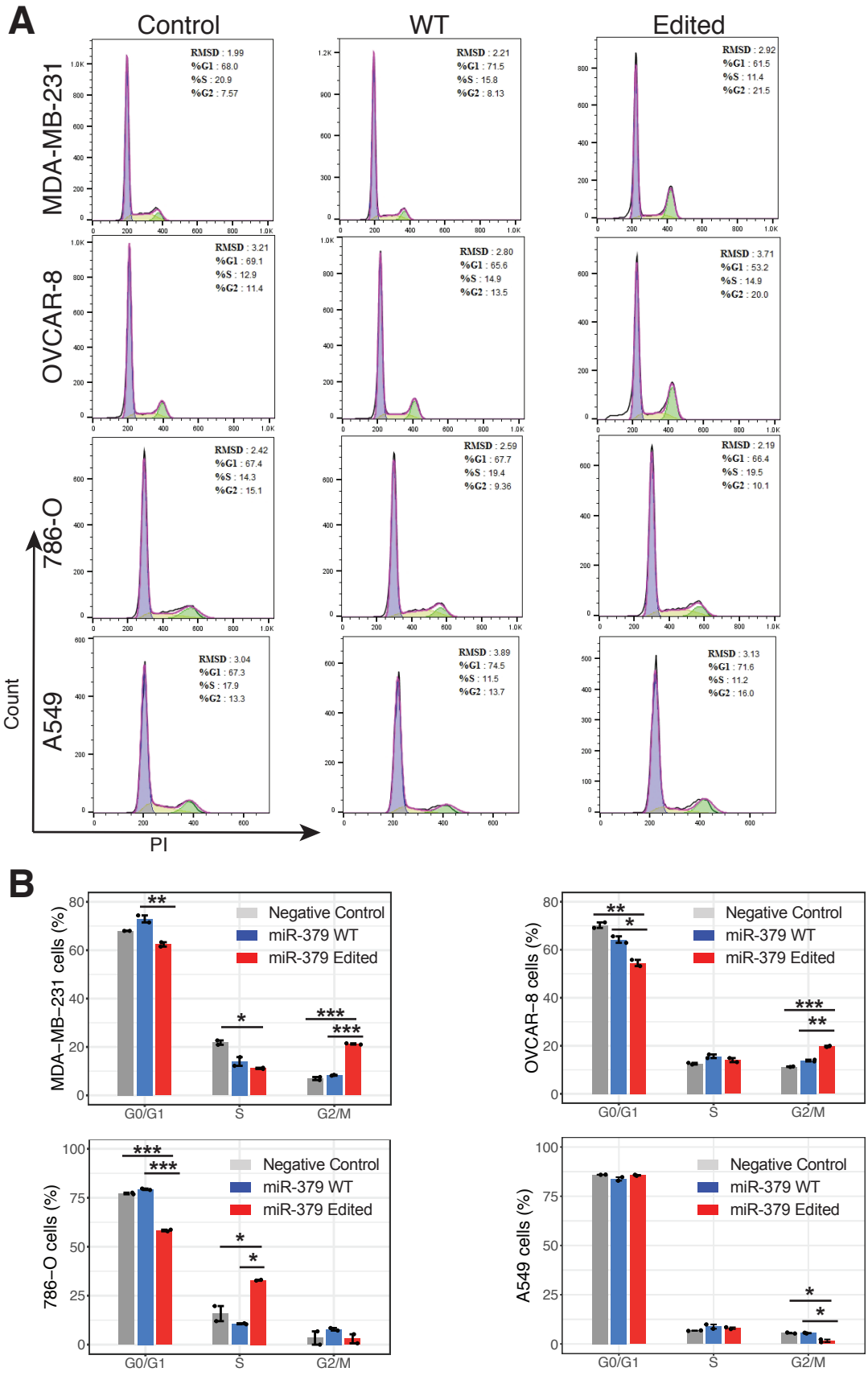

Supplemental Fig. 3. Effects of transfected miR-379-5p on cell cycle in MDA-MB-231, OVCAR-8, 786-O and A549 cells using flow cytometry

(A) Cell cycle analysis by PI staining. Representative traces from three different experiments are shown. (B) Percentage of cells in each phase was quantified using FlowJo software and is shown as the mean. Error bars indicate SD; ANOVA with Tukey's test as post-hoc test was used to assess the difference; $*p < 0.05$, $**p < 0.01$, $***p < 0.001$.

Figure S4

A

MDA-MB-231 (NES: 2.53, pvalue=0)

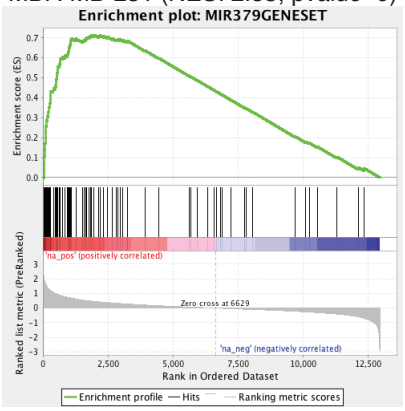

786-O (NES: 2.46, pvalue=0)

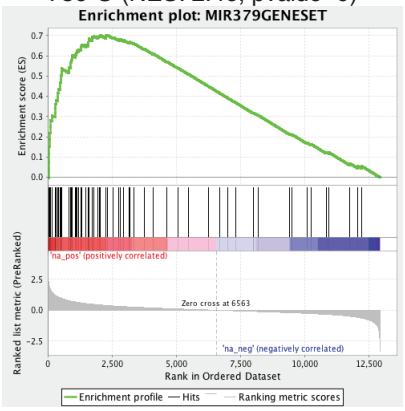

HeyA8 (NES: 2.45, pvalue=0)

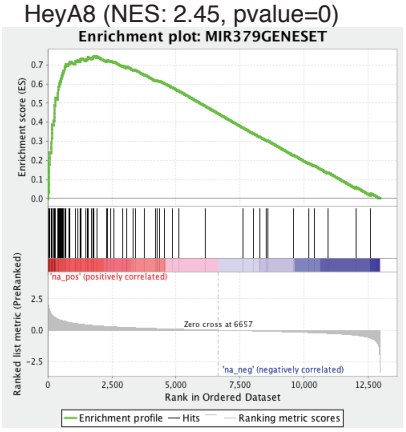

OVCAR-8 (NES: 2.43, pvalue=0)

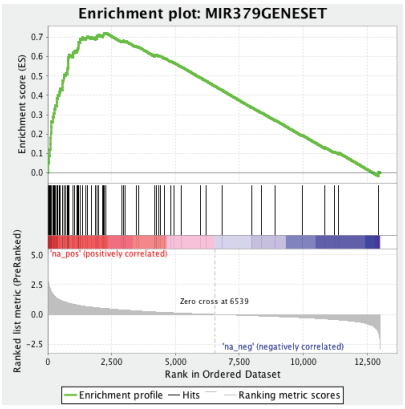

PC-3 (NES: 2.40, pvalue=0)

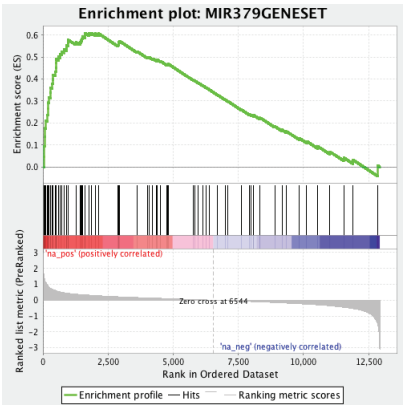

B

MDA-MB-231 (NES: 1.71, pvalue=1.68x10^{-3})

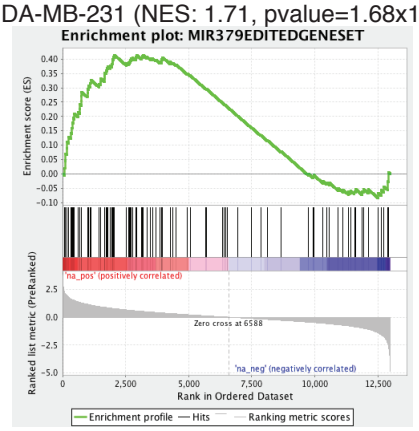

786-O (NES: 1.87, pvalue=0)

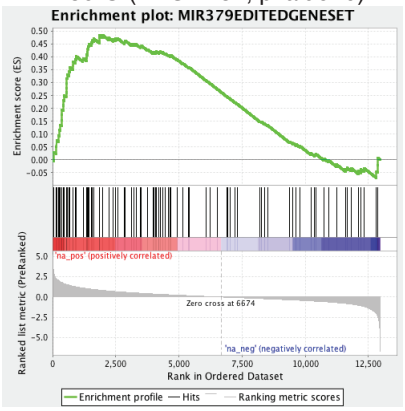

HeyA8 (NES: 2.31, pvalue=0)

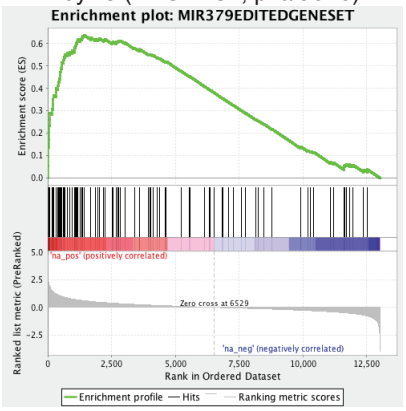

OVCAR-8 (NES: 1.78, pvalue=0)

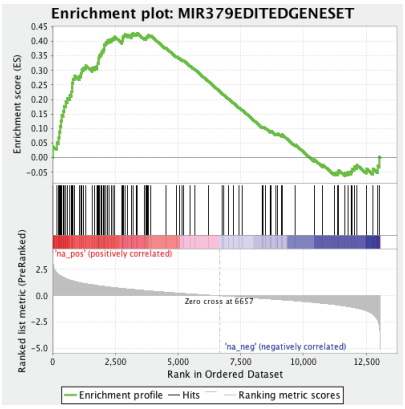

PC-3 (NES: 1.40, pvalue=1.6x10^{-2})

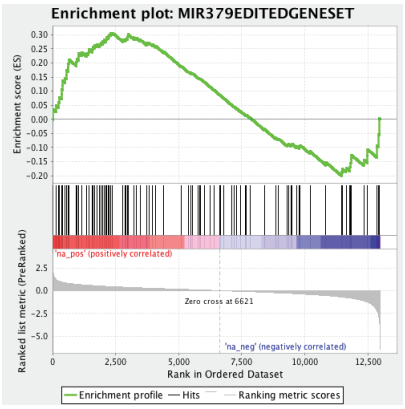

Supplemental Fig. 4. Enrichment of genes with the corresponding miR-379 binding motif in down-regulated genes upon transfection of WT miR-379 (A) and edited miR-379 (B) in 5 cancer cell lines.

Figure S5

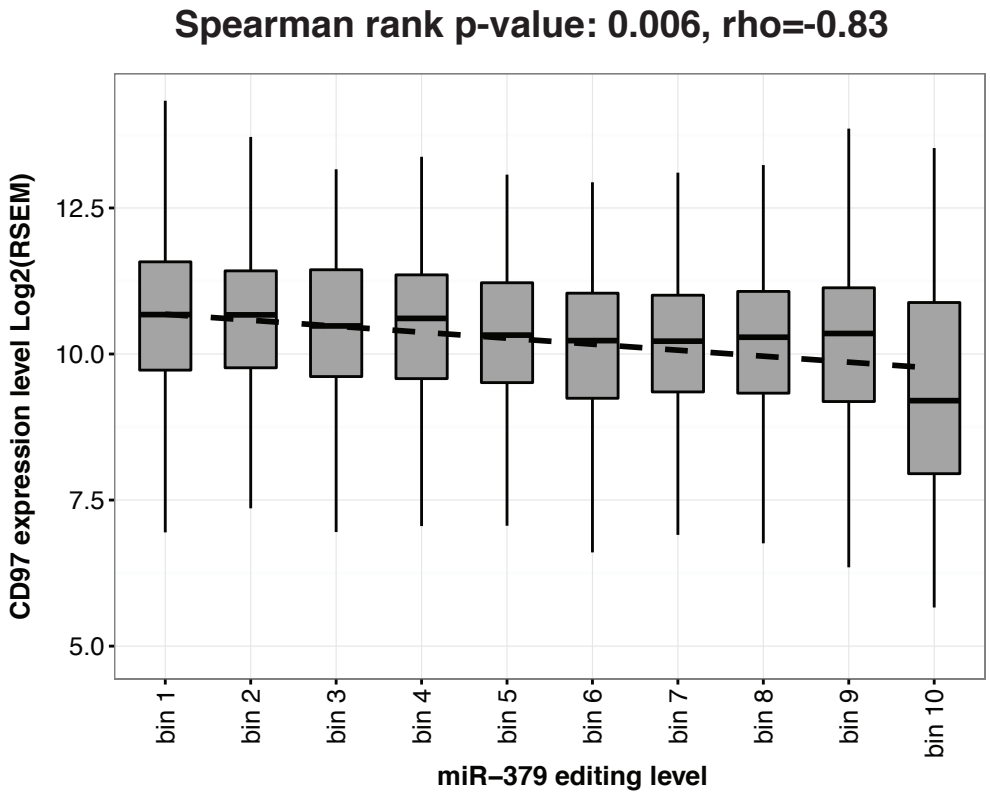

Supplemental Fig. 5. Correlation between miR-379-5p edited level and CD97 mRNA expression across cancer types

We split all TCGA patient samples into 10 equal bins based on their miR-379-5p editing level, and calculated the correlation between the median editing level and the median expression level of CD97. Spearman rank p value and correlation coefficient are shown.

Figure S6

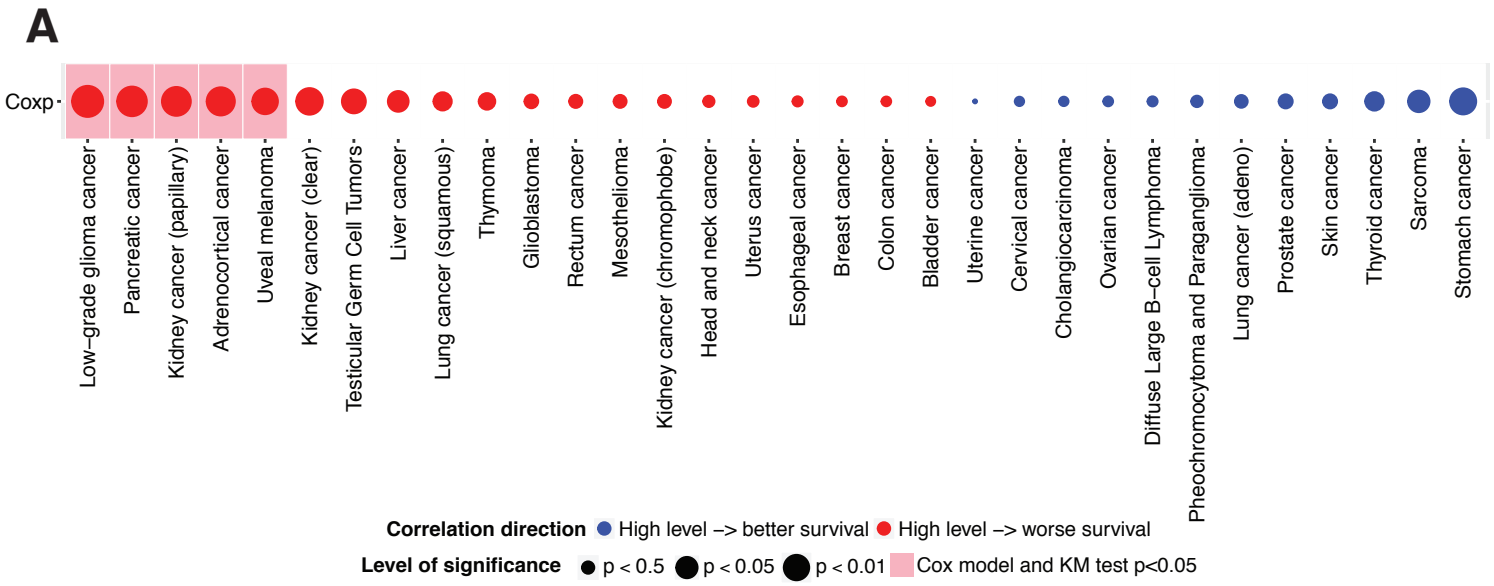

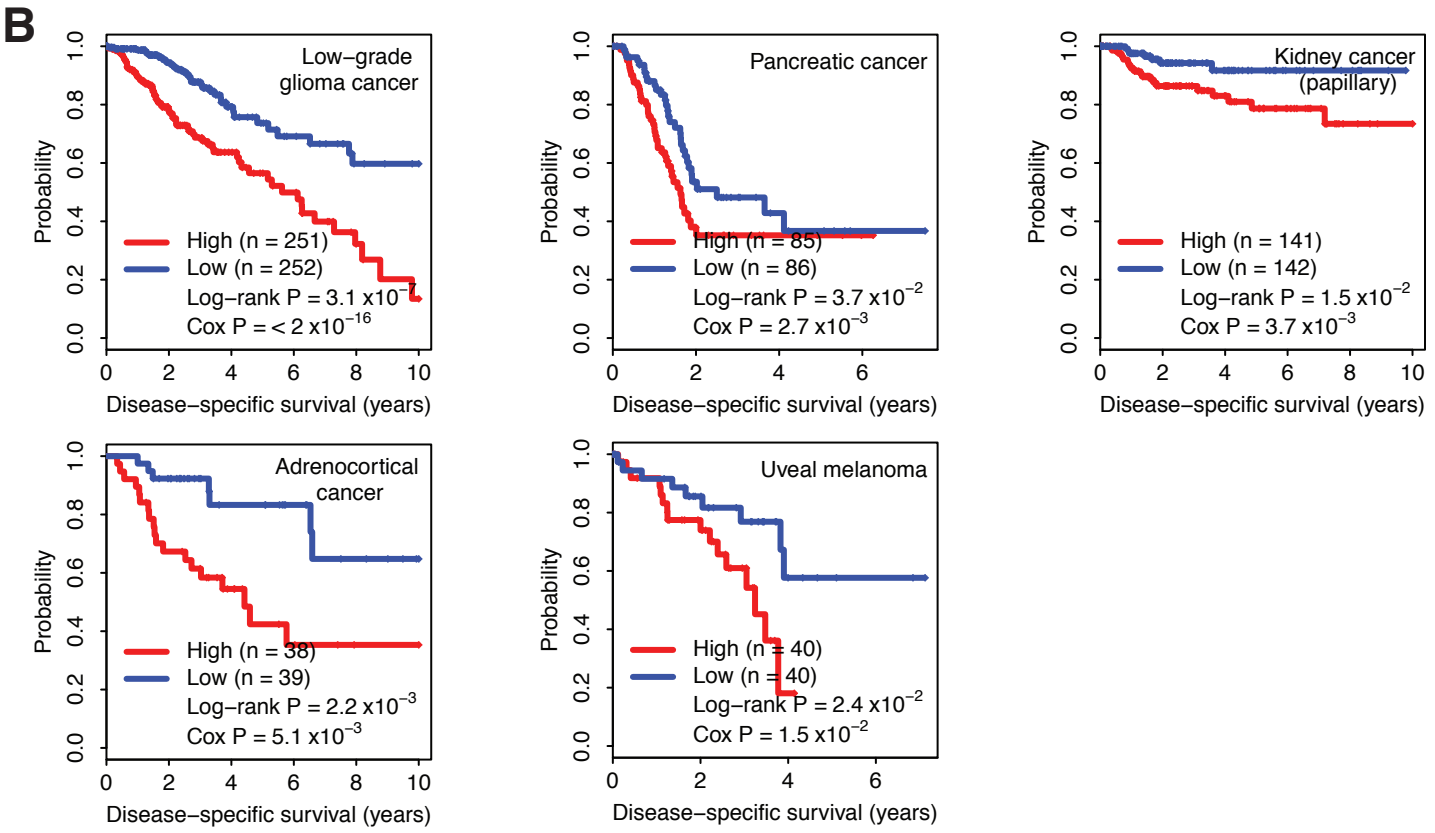

Supplemental Fig. 6. Clinically relevant patterns of CD97 mRNA expression in TCGA patient samples (A) Summary of Cox proportional hazard ratio model of CD97 mRNA expression level with patient disease-specific survival. Dot size indicates statistical significance level; color indicates correlation direction. Pink blocks highlight $p < 0.05$. (B) Significant survival correlations of CD97 mRNA expression with patient disease-specific survival times (separated by the median value) in different cancer types ($p < 0.05$); Cox p and log-rank p values are reported.

Figure S7

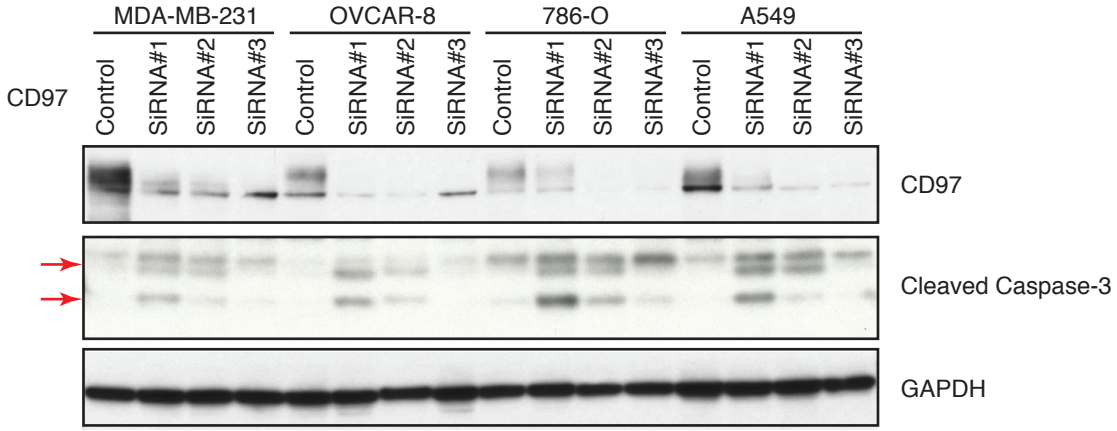

Supplemental Fig. 7. Knockdown effects of CD97 by three siRNAs validated by Western blots Western blots of CD97 and cleaved caspase-3 upon 72-hr transfection with CD97 siRNAs (#1, #2, and #3) in MDA-MB-231, OVCAR-8, 786-O and A549 cells. GAPDH was used as loading control.

Figure S8

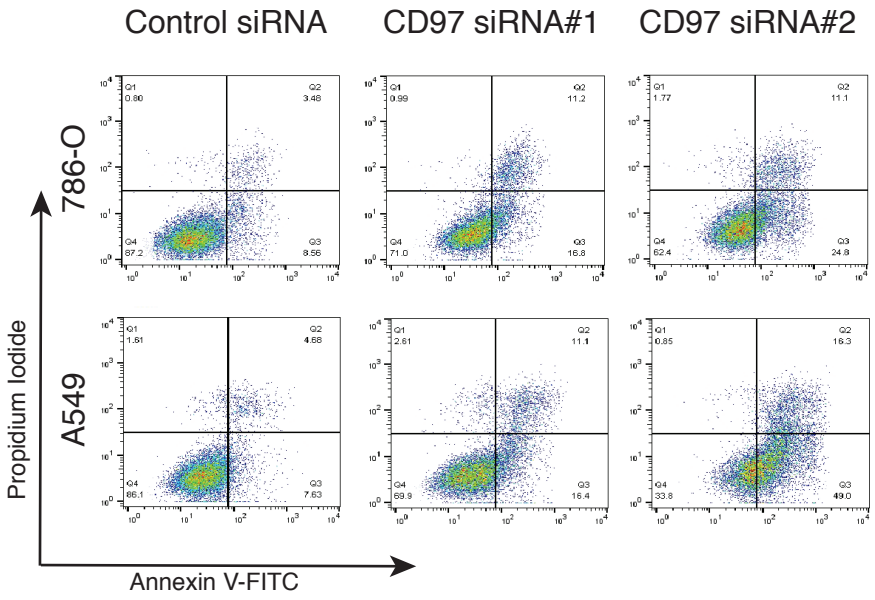

Supplemental Fig. 8. Effects of two CD97 siRNAs on cell apoptosis
Representative images of cell apoptosis after transfection of two CD97 siRNAs (#1 and #2) by AV-FITC/ PI staining in 786-O and A549 cells.

Figure S9

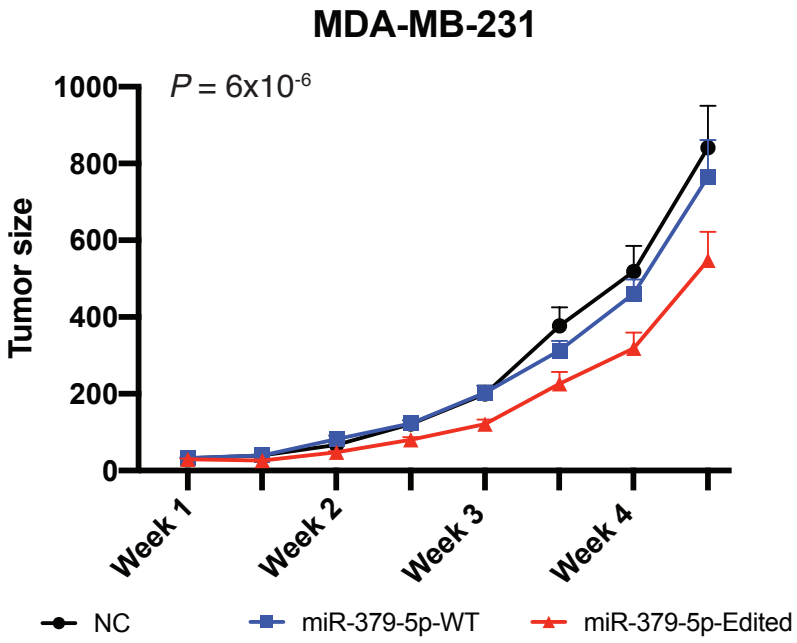

Supplemental Fig. 9. The effect of miRNA mimics on tumor size by caliper along time Tumor size (mean with SEM) was reported for the MDA-MB-231 mouse model. A two-way analysis of variance test was performed to evaluate the impact of time and different treatments. Each measurement was considered independent and treatment p value was reported.

Figure S10

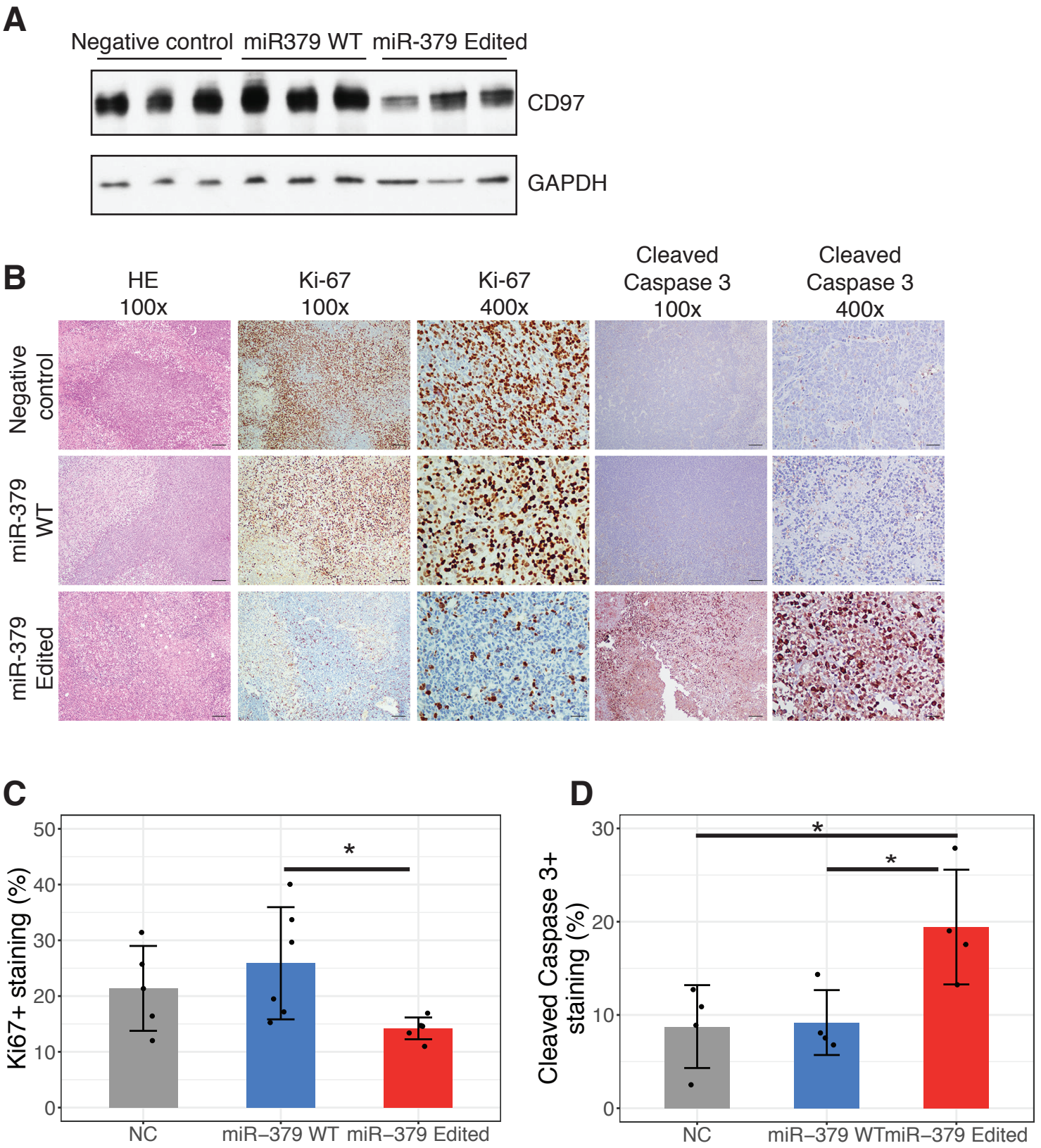

Supplemental Fig. 10. Representative images of tissue sections from mice
(A) Western blots of CD97 from tissue sections, and (B) hematoxylin & eosin staining of tumor sections and paraffin-embedded tumor tissue sections immunostained with Ki-67 proliferation marker, and cleaved caspase-3 apoptosis marker. Representative tumors are shown (scale bars: 100 μm). Original magnification, ×100 and ×400. (C) The relative positive rate of Ki-67 and (D) cleaved caspase-3 in tissue sections. Data show mean with SD; ANOVA with Tukey's test as post-hoc test was used to assess the difference; $^{*}p < 0.05$, $^{**}p < 0.01$, $^{***}p < 0.001$.

Table S1. Overview of TCGA miRNA sequencing data.

Cancer type	# Sample	Tumor sample	Normal sample	Average tumor mappable reads (millions)	Average normal mappable reads (millions)	# Confident A-to-I editing events
Bladder	414	395	19	5.96 ± 3.85	15.39 ± 9.99	929
Breast	890	801	89	3.76 ± 2.74	3.80 ± 2.49	2021
Cervical	301	298	3	5.33 ± 2.46	15.3 ± 1.74	682
Colon	399	391	8	4.48 ± 3.82	1.22 ± 0.36	883
Head and neck	562	518	44	5.05 ± 2.34	6.34 ± 2.13	1189
Kidney (chromophobe)	90	65	25	6.35 ± 1.60	8.08 ± 2.25	103
Kidney (clear)	587	516	71	3.57 ± 2.41	3.73 ± 1.39	1032
Kidney (papillary)	325	291	34	6.74 ± 2.94	9.00 ± 2.64	551
Leukemia	188	188	0	0.85 ± 0.31	NA	311
Low-grade glioma	511	511	0	2.41 ± 1.08	NA	2620
Liver	421	371	50	5.12 ± 2.27	5.53 ± 1.61	935
Lung (adeno)	529	483	46	5.47 ± 2.73	5.99 ± 2.75	1250
Lung (squamous)	519	474	45	3.83 ± 2.10	8.22 ± 2.88	1137
Ovarian	489	489	0	4.01 ± 1.99	8.34 ± 4.70	976
Prostate	545	493	52	6.71 ± 3.56	NA	1233
Rectum	160	157	3	5.32 ± 4.17	1.10 ± 0.34	347
Melanoma	100	98	2	4.20 ± 2.24	1.94 ± 0.11	219
Stomach	430	389	41	5.31 ± 4.16	9.70 ± 6.57	879
Thyroid	587	518	69	5.65 ± 2.09	7.16 ± 2.12	1057
Uterus	548	515	33	5.12 ± 3.74	16.69 ± 7.57	1092
Total	**8595**	**7961**	**634**	**4.76**	**7.50**	**19446**